The Journal of Experimental Biology 204, 3717–3726 (2001)
Printed in Great Britain © The Company of Biologists Limited 2001
JEB3752

Calcium currents from jellyfish striated muscle cells: preservation of phenotype, characterisation of currents and channel localisation

Y.-C. James Lin and Andrew N. Spencer*

Department of Biological Sciences, University of Alberta, Edmonton, Alberta, Canada T6G 2E9 and *Bamfield Marine Station, Bamfield, British Columbia, Canada V1R 1B0*

*Author for correspondence (e-mail: aspencer@bms.bc.ca)

Accepted 31 July 2001

Summary

When striated muscle cells of the jellyfish *Polyorchis penicillatus* were dissociated at 30 °C they retained their *in vivo* morphology and the integrity of ionic currents. This contrasted with cells dissociated at room temperature that rarely expressed any inward currents. Whole-cell, patch-clamp recordings from dissociated muscle cells revealed that the inward component of the total ionic current consisted of only one calcium current. This calcium current activated at −70 mV, peaked at −30 mV, and inactivated within 5 ms. In comparison with barium and strontium ions, calcium ions were the preferred current carriers. Calcium channels can be blocked by dihydropyridines and nickel ions at micromolar levels. Several properties of this current are reminiscent of T-type calcium currents. Localisation of this channel using the fluorescent channel blocker fDHP and the fluorescent dye RH414 indicated that myofibres had a higher density of these channels than the somata.

Key words: LVA calcium channel, striated muscle, jellyfish, voltage-clamp, dihydropyridine, Cnidaria, jellyfish, *Polyorchis penicillatus*.

Introduction

Calcium ions play an important role in regulating a number of cellular processes, with the calcium ion concentration in various compartments determining the onset, speed and termination of various biochemical and biophysical events (Berridge, 1993). Voltage-gated calcium channels play a crucial role since their activity will influence the cytoplasmic concentration of calcium ions. Among the numerous examples of the regulatory activity of Vg calcium channels are smooth and striated muscle contraction, transmitter release at synapses, signal transduction, development of vascular tone, release of hormones and cellular growth (Hille, 1992).

Voltage-gated calcium channels can be categorised into high-voltage-activated (HVA) and low-voltage-activated (LVA) channels. In general, HVA calcium channels activate above −40 mV. The activation and inactivation kinetics of HVA calcium channels are quite variable but they can be identified by their sensitivity to various pharmacological agents. They are categorised into at least five classes, namely L, N, P, Q and R types, based on their pharmacological properties. LVA channels activate at around −70 to −40 mV, inactivate rapidly, and are sensitive to nickel and mibefradil (Bean, 1985; Akaike et al., 1989; Huguenard, 1996; Ertel et al., 1997). To date, only one type of LVA channel has been identified, the T-type calcium channel.

Voltage-gated calcium channels are found in all muscle types; however, their roles in muscle contraction differ depending on the muscle type. Influx of external calcium ions is required to initiate contraction in both smooth and cardiac muscle but not in skeletal striated muscle of vertebrates (Bers, 1991), where depolarisation of the membrane triggers release of calcium from the sarcoplasmic reticulum (Endo, 1977). All cardiac myocytes possess L-type calcium channels, while T-type channels are also present in cardiac cells that display primary or secondary pacemaker activity such as at the sinoatrial node, sinus venosus and Purkinje fibres (Hagiwara et al., 1988; Hirano et al., 1989; Tseng and Boyden, 1989; Bois and Lenfant, 1991). However, T-type channels are absent or present at low densities in ventricular myocytes (Bers, 1991; Campbell and Strauss, 1995). Thus, the primary role of L-type calcium channels appears to be the control and modulation of the electromechanical coupling process, while T-type channels are involved in pacemaker activity.

Several voltage-gated calcium currents have been recorded from neurones in jellyfish (Mackie and Meech, 1985; Anderson, 1987; Przysiezniak and Spencer, 1992), smooth muscles in ctenophores (Bilbaut et al., 1988; Dubas et al., 1988), and fertilised eggs in ctenophores (Barish, 1984). Calcium currents are present in the striated swimming muscle of the medusa *Polyorchis penicillatus* (Spencer and Satterlie, 1981). More recently, using isolated striated muscle strips from this jellyfish, we have shown that contraction depends on extracellular calcium and can be inhibited by the calcium channel blocker nitrendipine (Lin et al., 2000). Using both electrophysiological techniques and specific labelling, we

report the presence of low-voltage-activated calcium currents in striated myocytes of the hydrozoan jellyfish *Polyorchis penicillatus*. Retention of functional channels in these cells required dissociation at 30 °C, with much of the current being lost at room temperature. A primary function of calcium currents through this channel population is to initiate muscle contraction. We have determined that the muscle feet have a far higher density of these channels than the somata.

Materials and methods

Collection

Medusae of *Polyorchis penicillatus* were collected from Bamfield Inlet or Pachena Bay, near Bamfield, BC, Canada, and maintained in an aquarium with running sea water (9–12 °C) at the Bamfield Marine Station, Bamfield, BC, Canada. The normal water temperature that these jellyfish experienced ranged from 7 to 20 °C throughout the year.

Cell dissociation and electrophysiology

Subumbrellar sections were excised from the whole jellyfish and the radial and ring canals trimmed away. The muscle layer was stripped off the endodermal lamella using a pair of forceps. One medium-sized jellyfish (about 15–20 mm in bell diameter) yielded approx. 200 µl of striated muscle cells with some mesoglea attached. The stripped tissues were put into a 1.5 ml Eppendorf tube and a digestion solution of 1 mg ml^{-1} Pronase (Boehringer Mannheim) dissolved in artificial sea water (ASW), either prewarmed to 30 °C or at room temperature (20–22 °C), was added to the Eppendorf tube to a final volume of 1 ml. Test tubes were left undisturbed at either room temperature (20–22 °C) or at 30 °C for 15–20 min. After digestion, a few gentle taps on the test tube was all that was needed to separate the tissue into single muscle cells. Muscle cells were dissociated at 30 °C because the contractile phenotype appeared to be fixed by heat. Muscle cells dissociated at 30 °C were easily identified by their long contractile processes, whereas muscle cells dissociated at room temperature could be identified by the lack of muscle feet and the retracted myofibres within the cytoplasm. Any remaining endodermal cells could be identified by their cuboidal or columnar shape. Before recording, cells were washed with the appropriate bath solution three times and resuspended in bath solution to a final volume of 500 µl.

Recordings were made immediately after dissociation. Each batch of cell suspension was used for about 3–4 h. One or two drops of cell suspension were added into a stagnant perfusion chamber and then cells were allowed to settle (some remained suspended) before recording.

Electrophysiological recording and data analysis followed the technique of Grigoriev et al. (Grigoriev et al., 1996). Briefly, whole-cell, tight-seal recordings were made using borosilicate glass pipettes (TW-150-4, World Precision Instruments), which were made on a Sutter automated puller, with resistances of 2–3 MΩ when filled with the pipette solution. Recordings were made with an Axopatch-1D amplifier (Axon Instruments), low-pass filtered at 3 kHz using a 4-pole Bessel filter, and digitised using a Labmaster TL-125 acquisition board (Axon Instruments). Individual cells were viewed under phase contrast with a Nikon Diaphot inverted microscope. A piezo-electric driver (Burleigh) was used to manipulate the pipette onto the cell surface. Perfusion with the relevant external recording solution started after successful seal formation. No contraction was observed during recording. Stimulus control, data acquisition and analyses were performed with pCLAMP 6.0 software (Axon Instruments) on a Dell personal computer. Leakage and capacitative currents were subtracted, prior to test pulses, using −P/4 or −P/5 protocols from a holding potential of −80 mV (pCLAMP 6.0). Series resistance (R_s) was compensated optimally to minimise voltage errors, and was usually set to values of ≥80 %. C_m (membrane capacitance) and R_s were obtained by minimising the capacitative transient in response to a hyperpolarising voltage step. Mean R_s was 4.39±0.81 MΩ (N=20) before compensation, and mean C_m was 5.49±1.07 pF (N=20) before compensation. All experiments were carried out at room temperature (20–22 °C).

Solutions

Before use all recording solutions were filtered through cellulose acetate membrane cartridges with a 0.2 µm pore size. ASW at pH 7.5 contained: NaCl 376 mmol l^{-1}, $Na_2(SO_4)$ 26 mmol l^{-1}, $MgCl_2$ 41.4 mmol l^{-1}, $CaCl_2$ 10 mmol l^{-1}, KCl 8.5 mmol l^{-1} and *N*-2-hydroxy-ethylpiperazine-*N*′-2-ethanesulphonic acid (Hepes) hemisodium salt 10 mmol l^{-1}. The bath solution at pH 7.5 contained: $MgCl_2$ 40 mmol l^{-1}, $CaCl_2$ (or $BaCl_2$ or $SrCl_2$) 10 mmol l^{-1}, KCl 15 mmol l^{-1}, N-methyl glucamine-HCl (NMG-Cl) 429 mmol l^{-1}, Hepes (free acid) 10 mmol l^{-1}. The pipette solution (pH 7.5) used for recording total membrane currents contained: NaCl 50 mmol l^{-1}, $MgCl_2$ 2 mmol l^{-1}, $CaCl_2$ 1 mmol l^{-1}, ethylene glycol-bis(β-aminoethyl ether)-*N*,*N*,*N*′,*N*′-tetraacetic acid (EGTA) 11 mmol l^{-1}, KCl 350 mmol l^{-1}, KOH 30 mmol l^{-1}, Hepes (free acid) 10 mmol l^{-1}. The pipette solution (pH 7.5) used for isolating calcium currents contained: NaCl 50 mmol l^{-1}, $MgCl_2$ 2 mmol l^{-1}, $CaCl_2$ 1 mmol l^{-1}, EGTA 11 mmol l^{-1}, CsCl 350 mmol l^{-1}, CsOH 30 mmol l^{-1}, Hepes (free acid) 10 mmol l^{-1}, TEA-Cl 20 mmol l^{-1}. Using the latter pipette solution all outward currents were blocked totally within the first minute after break-through.

Pharmacology of muscle contraction

The considerable thickness and elasticity of the mesoglea in the bell region made muscle tension recordings from this region extremely variable. A preliminary study indicated that muscle strips from bell regions and vela (the shelf of tissue at the opening of the bell) had similar pharmacologies. Therefore we used muscle strips from vela, which had a thin lamina of mesoglea, to measure tension development. The vela of medusae, anaesthetised in 1:1 isotonic $MgCl_2$ (0.33 mol l^{-1}) and ASW, were excised so as to provide continuous strips of maximal width. Care was taken not to include portions of the

innervating motor-neurone network in the strips by bisecting the strip lengthwise and using only the half closest to the free margin. The free ends of each velar strip were pinned to the Sylgard base of a 35 mm Petri dish, which also contained a pair of embedded $Ag/AgCl_2$ stimulating electrodes connected to a Grass S44 stimulator. The velar strip ran between the two stimulating electrodes and around a small hook attached to a capacitative force transducer (Kent Scientific Corporation). Tension on the strip was adjusted using a micromanipulator so as to remove any slack in the muscle strip. Repetitive square pulses of 30 ms duration and 0.2 Hz were given to produce a train of twitch contractions that did not show fatigue. The stimulation voltage was determined by increasing the voltage until no increase in the amplitude of contraction at the stimulation frequency of 0.1 Hz occurred. The voltages used usually were between 30 and 40 V. Perifusion was by a peristaltic pump at 1.5 ml min^{-1} and the perifusate was removed by vacuum. All perifusates were kept at 12–14 °C during the experiment by running part of the perfusion tubing through an ice bucket. Transduced tension was recorded on a digital, Dash-IV pen-recorder (Astro-Med Inc.). The amplitude of contractile force for each condition (control, drug effect and wash) was calculated by averaging 30 individual twitch contractions.

Localisation of calcium channels

The method used to localise calcium channels using dihydropyridine-BODIPY (fDHP) followed the protocol of Schild et al. (Schild et al., 1995), with some modification. Dissociated cells were incubated with both fDHP and the styryl dye, RH414 (Molecular Probes, Inc.) at final concentrations of 10 μmol l^{-1} and 5 μmol l^{-1}, respectively, for 15 min at room temperature before examination. A laser-scanning, confocal microscope (Molecular Dynamic, Inc.) was used to examine the spatial distribution of calcium channels. The wavelength of the excitation beam was set to 488 and 568 nm (argon ion laser, 4.0 mW). The emitted fluorescence from labelled cells was split by a dichroic mirror (565 nm) into two wavelength bands. The intensities of the green (fDHP) and red (RH414) fluorescent labelling were recorded by two photomultipliers with cut-off filters at 530 and 590 nm, respectively.

To calculate the ratio of fluorescence intensity between green (fDHP) and red (RH414), each confocal image was split into two grey-scale images registering green and red fluorescence intensity. Images were then generated by determining the ratio of the intensity of green fluorescence (fDHP) to that of the red fluorescence (RH414) using the image math function in 'NIH image software' (National Institute of Health, USA at http://rsb.info.nih.gov/nih-image/about.html). Only optical sections, 1 μm thick, with sharp and definitive membrane labelling by RH414 (red images) were used for data analysis as this indicated a perpendicular section through the cell membrane. Data were collected and measured using the tool function in NIH image software by drawing lines along the membrane where RH414 showed sharp and definitive labelling. Unless otherwise stated, results are expressed as mean ± S.E.M.

Results

Cell dissociation

The subumbrellar, muscle sheets of hydromedusae are formed by a monolayer of striated muscle cells. Each cell is polarised with contractile 'feet', containing the myofibrils, attached by a narrow neck to the cell soma where the nucleus and other organelles are located (Spencer, 1979). Cell dissociation at room temperature resulted in all cells having their muscle feet retracted with obvious striated myofibrillar bands within the cytoplasm (Fig. 1A), whereas cells dissociated at 30 °C preserved their polarised morphology with about 53±5 % of muscle cells having two pairs of muscle feet (Fig. 1B,C). Whole-cell recordings showed that cells

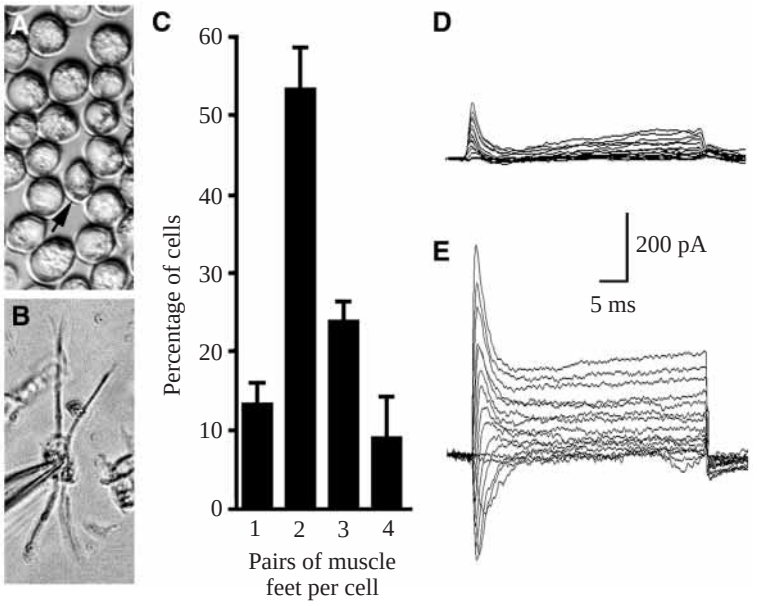

Fig. 1. Morphology of striated muscle cells dissociated from *Polyorchis penicillatus* at different temperatures and their associated membrane currents. (A) Phase-contrast micrograph of muscle cells dissociated at 20–22 °C showing that cells lose muscle feet and round up. Arrow indicates one tear-shaped cell with a remnant of myofibres. (B) Phase-contrast micrograph of muscle cells dissociated at 30 °C showing a muscle cell with two pairs of feet and a patch-recording pipette attached. (C) Histogram to show that muscle cells dissociated with 1 mg ml^{-1} Pronase at 30 °C retain their *in situ* morphology with 84.51±6.80 % of cells having two or more pairs of muscle feet (myofibres). Values are means ± S.E.M. (D) Voltage-clamp recording of total membrane currents from a cell dissociated at 20–22 °C showing that both inward and outward current amplitudes are low. The stimulus protocol was 25 ms test pulses, incrementing in 10 mV steps from –70 to +90 mV from a holding potential of –80 mV. (E) Voltage-clamp recording of total membrane currents from a cell dissociated at 30 °C showing increased amplitude of the currents. Stimulus protocol as for D.

dissociated at 30 °C not only retained their polarised morphology but also had more active voltage-gated channels as judged by current amplitude (Fig. 1D,E). Of the 87 heat-treated cells we examined, 75 had inward currents, whereas only four of the 20 cells dissociated at room temperature had inward currents. Occasionally some muscle cells that were dissociated at room temperature were tear-shaped with remnants of the muscle feet (Fig. 1A, arrow). All four cells that had some inward current after being dissociated at room temperature were tear-shaped.

Calcium-selective inward current

In the following experiments all cells were dissociated at 30 °C. Calcium currents were isolated by blocking the outward potassium current with Cs^{2+} and TEA applied intracellularly through the patch-pipette. Contamination by sodium currents was checked by using a calcium-free bath solution in which calcium ions and a portion of the NMG-Cl were replaced by 50 mmol l^{-1} EDTA-Na_2 or 100 mmol l^{-1} NaCl. In both cases Na^+ concentration was raised to 100 mmol l^{-1}. We only observed inward current in the calcium-free solution containing EDTA (N=4), not in the absence of EDTA (N=5). This confirmed the presence of calcium channels but not sodium channels. In this case the inward current, in a calcium-free bath solution, was carried by sodium ions passing through calcium channels, while in the absence of EDTA calcium channels were blocked by Mg^{2+} and no inward current was recorded. Fig. 2A shows a typical series of traces of an isolated strontium current. The channels carrying this current activated at approximately −70 mV with maximal current at −30 mV (Fig. 2B, N=10). Current density was calculated to be 0.18±0.05 mA cm^{-2} (N=20) by using the maximum current at −30 mV and whole cell capacitance (5.49±1.07 pF; N=20), assuming that membrane capacitance was 1 μF cm^{-2}. No reversal potential could be detected using test pulses up to +90 mV.

The ionic permeability of calcium channels to barium and strontium was measured (current traces not shown). Channels were equally permeable to barium and strontium with P_{Ba}/P_{Ca}=0.86±0.08 and P_{Sr}/P_{Ca}=0.85±0.05; N=4 cells in each case.

Electrical and kinetic properties

The rate of activation was voltage-dependent (Fig. 3A) with the time-to-peak for maximal current of 1.49±0.23 ms at −30 mV (N=10). The time course for inactivation was also voltage-dependent (Fig. 3B) with the inactivation time constant varying between 1.5 ms at +80 mV and 3.5 ms at −70 mV (N=10).

Fig. 4A shows the steady-state inactivation curve for Sr^{2+} current. The current was almost fully available at −100 mV, half inactivated at −80±3.5 mV, and completely inactivated at −45 mV. The time constant for recovery from inactivation was 51±0.8 ms (N=10) and complete recovery occurred in 200 ms (Fig. 4B).

Pharmacology of muscle contraction

We encountered severe channel run-down during recording so that in most cases no current could be recorded 5 min after starting test protocols. Attempts to decrease run-down by addition of ATP and GTP to the electrode solution were not successful. For this reason the selectivity of calcium channel blockers was first examined by evaluating their effect on contraction of muscle strips using field stimulation. When stimulated at 0.2 Hz at 12–14 °C in ASW these preparations could maintain a constant contractile force for several hours. Muscle contractile force was decreased in the presence of both dihydropyridines (DHP) and verapamil (Fig. 5). The dihydropyridines nicardipine and nifedipine completely inhibited contraction at concentrations of about 100 μmol l^{-1}, whereas other dihydropyridines, (+) and (−) Bay K 8644 and nitrendipine, completely inhibited contraction at concentrations less than 40 μmol l^{-1} (Fig. 5). Diltiazem at 100 μmol l^{-1} and DMSO at 0.5 % had no effect (data not shown).

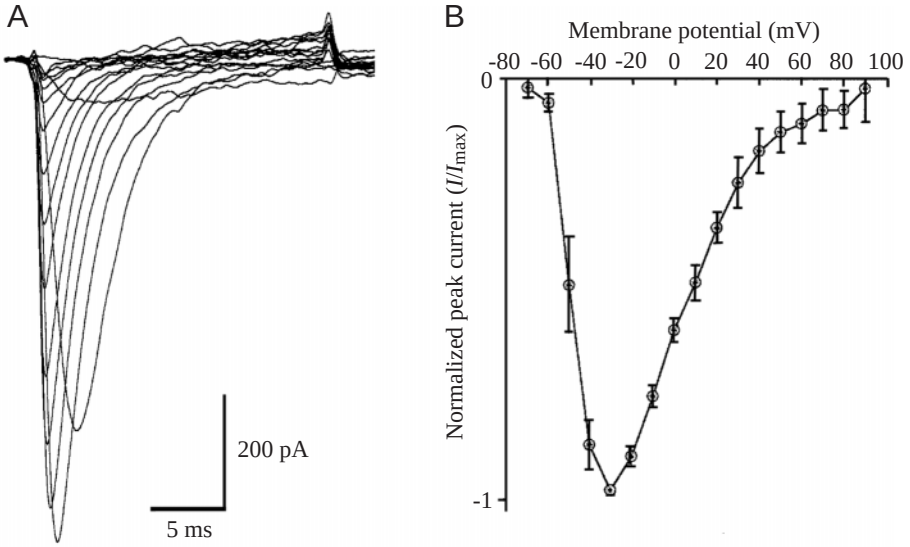

Fig. 2. Low-voltage-activated calcium current recorded from a muscle cell dissociated at 30 °C. (A) Current traces recorded in whole-cell, voltage-clamp mode using a bath solution where calcium was replaced by 50 mmol l^{-1} $SrCl_2$ to prevent run-down of this current. All potassium currents were blocked by CsOH, $CsCl_2$ and TEA-Cl in the pipette solution (see Materials and methods). The stimulus protocol was a series of 25 ms test potentials with increments of 10 mV from −70 to +90 mV using a holding potential of −80 mV. (B) Mean I/V curve from 10 cells using the above protocols. Values are means ± S.E.M.

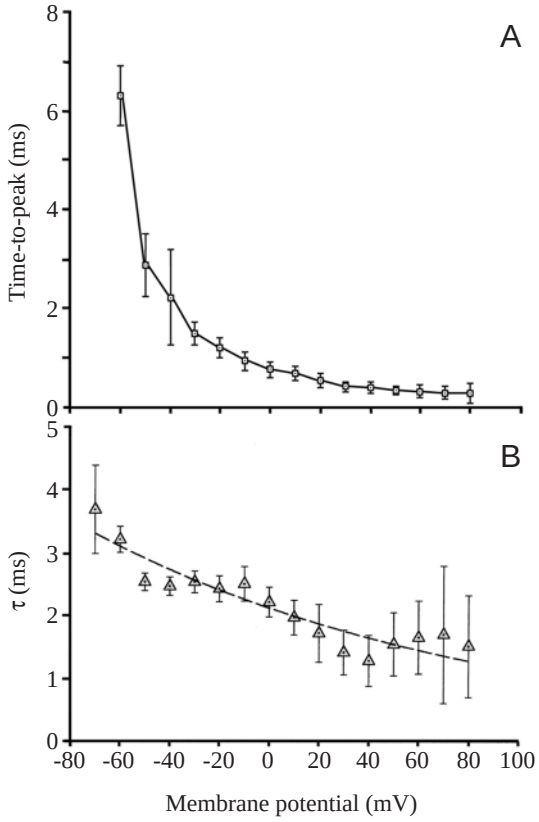

Fig. 3. Voltage dependence of time-to-peak (A) and inactivation time constant (τ; B) of the low-voltage-activated calcium current. Sr^{2+} was used as the charge carrier. The stimulus protocol for both graphs was a series of 25 ms test pulses with increments of 10 mV from −70 to +90 mV from a holding potential of −80 mV. The time constant (τ) for the inactivation decay was obtained by fitting the calcium current decay with a single exponent at each testing potential using the Clampfit program (Axon Instruments). The means from each testing potential were fitted with Sigma Plot 4.0 program (SPSS Inc.). Values are means ± S.E.M., N=10 cells.

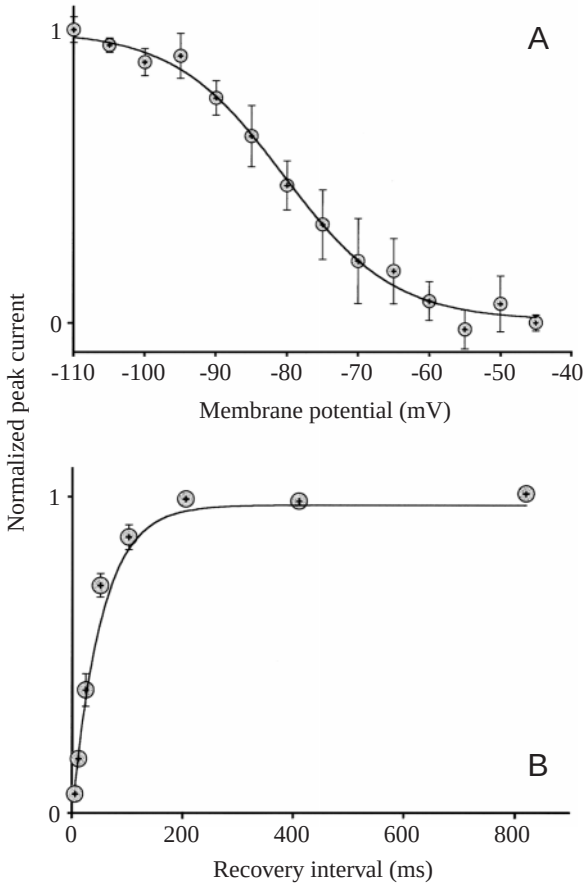

Fig. 4. Steady-state inactivation and recovery from inactivation of the low-voltage-activated calcium current. Sr^{2+} was used as the charge carrier. (A) The steady-state inactivation curve was obtained from data generated using 20 ms test pulses to −30 mV immediately following 2 s conditioning prepulses in 5 mV increments from −110 to −30 mV. The holding potential prior to the conditioning pulse was −80 mV. Steady-state inactivation data were normalised to averaged maximal current (I/I_{max}) and the means fitted with a Boltzman equation ($I/I_{max}=1/\{1+\exp[(V_{pp}-V_{50})/k]\}$, where V_{pp} is the prepulse voltage, V_{50} is the prepulse voltage causing half-inactivation; k is the slope factor of the inactivation curve in mV per e-fold change). V_{50}=−80±3.5 mV, k=7.7±1.9 mV, N=7. (B) The curve for recovery from inactivation was generated from data obtained using 20 ms inactivating prepulses to −30 mV from a holding potential of −80 mV, followed by a recovery period (R_t) of variable duration from 6.4 to 800 ms at −80 mV, and a 25 ms test pulse to −30 mV. Peak currents obtained in response to test pulses were normalised to prepulse values (I/I_{max}) and fitted with exponential curves ($I/I_{max}=1-\exp(-R_t/\tau)$, where R_t is the recovery period and τ is the time constant). τ=51.7±0.8 ms. Values are means ± S.E.M., N=10.

Pharmacology of LVA channels in dissociated cells

The effect of dihydropyridines on dissociated cells was also examined to see if blockade of T-type calcium channels could account for the loss of contractility. Only the doses that gave complete inhibition of muscle contraction were used. Fig. 6 shows typical traces of the inhibitory effects of nifedipine at 100 μmol l^{-1} (76.08±4.60 %, N=4), nitrendipine at 40 μmol l^{-1} (78.02±5.41 %, N=3), (+) Bay K 8644 at 20 μmol l^{-1} (81.37±4.56 %, N=5), verapamil at 100 μmol l^{-1} (78.22±3.20 %, N=3), and $NiCl_2$ at 50 μmol l^{-1} (57.28±6.00 %, N=4).

Localisation of LVA channels by fDHP

Because larger amplitude membrane currents were recorded from dissociated cells that had been heat-treated, and since they also retained muscle feet, we surmised that there was a differential pattern of channel distribution over the cell surface, with channels being preferentially inserted in, or migrating to, the membrane overlying the muscle feet. We used fDHP to label calcium channels since we had determined that these channels were blocked by DHPs. RH414 was used as a reference dye to correct for possible artefacts caused by membrane topology. Fig. 7A shows double-labelling of muscle cells dissociated at room temperature with fDHP (green) and RH414 (red). These cells became spherical, with RH414 labelling only the plasma membrane while fDHP labelled mostly small vesicles within the cytoplasm though

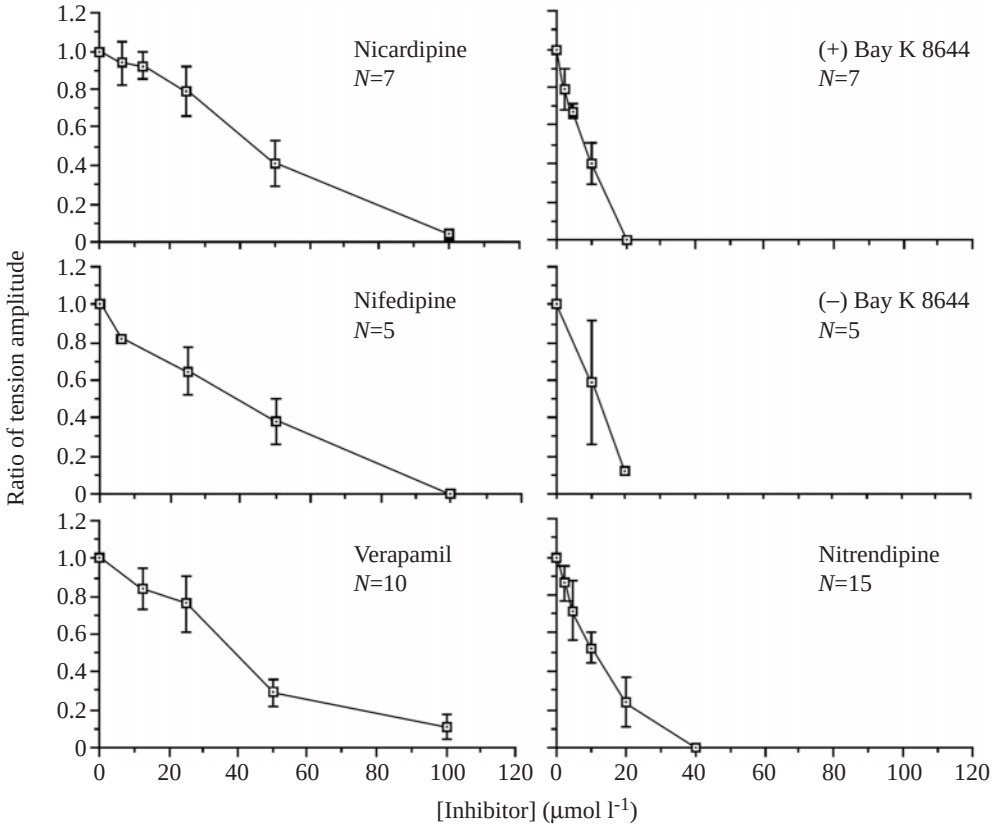

Fig. 5. Effect of various dihydropyridines and verapamil on muscle contraction. Velar strips were subjected to field stimulation at 0.2 Hz for 30 ms. Mean peak tension was registered on a digital pen recorder through a capacitative force transducer. Peak tension was normalised to that in the ASW control. The perifusion rate was set at 1.5 ml min^{-1} and the temperature of the perifusate was 10–12 °C. Values are means ± S.E.M.

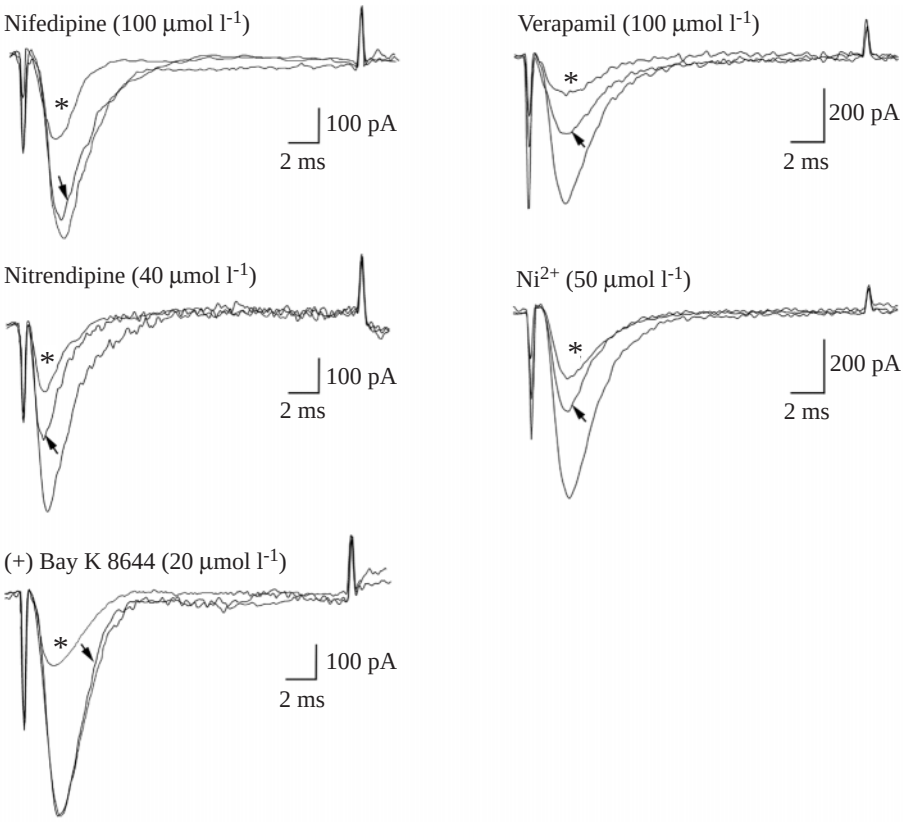

Fig. 6. Effect of dihydropyridines, verapamil and $NiCl_2$ on the low-voltage activated calcium current of muscle cells. Sr^{2+} was used as the charge carrier. Unmarked traces are those recorded before the drug was applied while traces marked with an asterisk indicate those recorded with the drug applied, and traces marked by an arrow indicate those recorded after washing with bath solution. The stimulus protocol used was a single 20 ms voltage step to −30 mV from a holding potential of −80 mV. The early large phasic negative-going current excursion is the uncompensated capacitative current while the transients at the end of the traces are the 'off' capacitative transients.

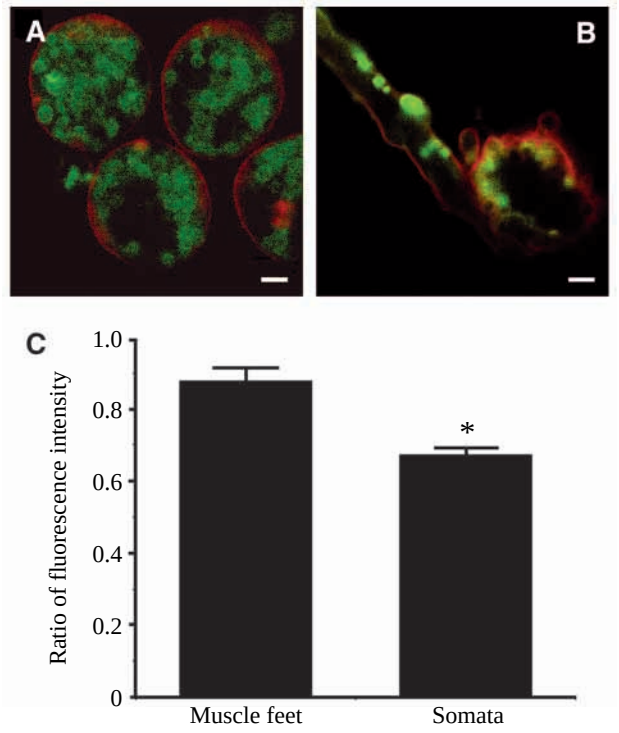

Fig. 7. Localisation of calcium channels using dihydropyridine-BODIPY (fDHP) and RH414 in striated muscles dissociated at room temperature (20 °C; A) and at 30 °C (B). Dissociated cells were incubated with both fDHP (final concentration 10 μmol l^{-1}) and the styryl dye RH414 (final concentration 5 μmol l^{-1}), for 15 min at room temperature before examination. Images were obtained using laser-scanning, confocal microscopy. The wavelengths of the excitation beam were set to 488 nm and 568 nm. The emitted fluorescence from labelled cells was collected at 530 nm for green fluorescence (fDHP) and 590 nm for red fluorescence (RH414). At 20 °C cells were spherical and fDHP labelled mostly small vesicles within the cytoplasm (A) while at 30 °C there was strong fDHP labelling of the sarcolemma of the muscle feet (B). Scale bars, 2 μm. (C) Ratio of labelling intensity of green (fDHP) *versus* red (RH414) fluorescence in the plasma membrane of myofibres (feet) and the cell somata. Data on the intensity of fluorescence (both green and red) were collected from those areas of the membrane showing sharp and definitive RH414 labelling (red), indicating that a perpendicular optical section through the cell membrane was being analyzed. The intensity of green fluorescence (fDHP) was divided by the intensity of red fluorescence (RH414) pixel-by-pixel using NIH image software. Values are means ± S.E.M., N=20 cells. Asterisk, significant difference (P<0.05).

occasionally fDHP labelling could be seen on the membrane. Fig. 7B shows double-labelling of muscle cells dissociated at 30 °C, which always showed both RH414 and fDHP labelling. There was an obvious association of fDHP labelling with the sarcolemma of the muscle feet. To analyse the differential distribution pattern of fDHP labelling, the ratio of the intensity of green *versus* red fluorescence of images was measured pixel-by-pixel using NIH imaging software. Larger ratios indicated a higher density of fDHP labelling. The ratio of labelling intensity (fDHP to RH414) in the sarcolemma around the muscle feet was significantly higher than the somatal membrane (0.88±0.03 and 0.67±0.02, respectively, P<0.05, N=20 cells; Fig. 7C).

Discussion

Cell dissociation and phenotype fixation

Our data suggest that heat treatment 'locks' the cytoskeleton, thereby 'fixing' cell morphology after dissociation. Heat treatment has been used previously during dissociation of tissues from other marine hydrozoan medusae and polyps for the purpose of cell identification (Schmid et al., 1981; Plickert and Kroiher, 1988). Like Schmid and colleagues (Schmid et al., 1981), we noticed that there was a relatively short window of time and temperature for heat 'fixation' of the cellular phenotype, and this was particularly the case for retention of electrophysiological competence. Prolonged treatment at 30 °C (>30 min) or treatment at a higher temperature (37 °C) for 15 min preserved cell morphology, but ionic currents could not be recorded. Heat treatment did not apparently alter the kinetics of the inward current, since when compared with cells dissociated at room temperature qualitatively similar kinetics were observed, though current amplitude was markedly reduced (Lin et al., 2000). Inward currents were so small after dissociation at 20 °C that statistically relevant data could not be obtained.

Channel localisation and fixation

Since only cells with intact feet showed large currents, it is possible that most of the channels are located on the feet. Our fDHP data also support the proposition that DHP-sensitive ion channels are at a higher density on the feet. Several other excitable cells also show a differential distribution pattern of ion channels that are obviously related to the excitability properties of the cell in question. For example, voltage-gated sodium channels are known to be clustered at the nodes of Ranvier in vertebrate myelinated axons and neuromuscular junctions (Ritchie and Rogart, 1977; Ellisman and Levinson, 1982; Lupa and Caldwell, 1994), and L-type calcium channels are known to aggregate in T-tubules (Carl et al., 1995). Jellyfish striated muscle cells are morphologically separated into a somal and a 'foot' region (Spencer, 1979). These muscle feet contain the contractile myofibres that use extracellular calcium during excitation–contraction coupling (Spencer and Satterlie, 1981). Localisation of calcium channels on muscle feet in jellyfish striated muscle is further supported by the presence of membranous calcium stores just beneath the membrane of muscle feet (Lin and Spencer, 2001). A close association between calcium channels and calcium stores would allow for possible direct electrical coupling or calcium-induced calcium release to augment the influx of calcium through voltage-gated channels for regulation of muscle contraction. The precise way ion-channel proteins and the cytoskeleton interact mechanically is not known, especially for jellyfish. Nevertheless, several adapter proteins have been reported to be associated with voltage and ligand-gated ion

channels, which link them to the cytoskeleton. For example, ankyrin and spectrin immobilise sodium channels with actin filaments at presynaptic terminals and along axons (Srinivasan et al., 1988), while rapsyn links nicotinic acetylcholine receptors to actin filaments at neuromuscular junctions (Apel et al., 1995) and gephyrin links glycine receptors to microtubules at postsynaptic sites (Kirsch et al., 1993). $GABA_A$-receptor-associated protein (GABARAP) links $GABA_A$ receptors to microtubules at synapses (Wang et al., 1999).

Channel kinetics

The electrophysiological characteristics of the calcium currents recorded from isolated jellyfish muscle cells are similar to those of T-type currents: activation occurred at low voltages (−70 mV), with both activation and inactivation being very rapid and voltage-dependent. Moreover, this current showed another characteristic of T-type channels (Randall and Tsien, 1997) wherein, with progressively stronger depolarisations, successive currents activated and inactivated faster. A noticeable difference between the current we recorded and T-type currents in other systems was the greater rate of both activation and inactivation in jellyfish muscle cells. Time-to-peak for maximum current at a membrane potential of −30 mV was 1.49±0.23 ms and the inactivation time constant was 2.59±0.38 ms for the calcium currents recorded from jellyfish muscles. In comparison the activation time constants for most other T-type currents are usually greater than 10 ms, with inactivation constants greater than 20 ms (Huguenard, 1996; Randall, 1998; Randall and Tsien, 1997).

Pharmacology

Our experiments examining the effects of various known calcium channel blockers on muscle contraction were an indirect method for evaluating channel properties, but they also provide us with estimates of the doses that might be effective when using whole-cell, patch-clamp recording. Although dihydropyridines are known to have higher inhibitory potency for L-type calcium channels than T-type channels (Hille, 1992), the sensitivity of the jellyfish calcium current to dihydropyridines, with an IC_{50} in the $\mu mol\,l^{-1}$ range, was similar to that reported for T-type calcium channels found in some vertebrate cells, including mouse spermatocytes (Arnoult et al., 1996; Lievano et al., 1996; Santi et al., 1996), hippocampal CA1 neurones (Takahashi and Akaike, 1991), cerebellar Purkinje cells (Kaneda et al., 1990), amygdaloid neurones (Kaneda and Akaike, 1989), rat hypothalamic neurons (Akaike et al., 1989) and mouse sensory neurones (Richard et al., 1991). LVA T-type calcium currents have been reported in some excitable cells of invertebrates (Hagiwara et al., 1975; Deitmer, 1984; Yamoah and Crow, 1994; Ödblom et al., 2000), where the LVA calcium currents in cardiac myocytes of squid are shown to be sensitive to dihydropyridines at micromolar levels (Ödblom et al., 2000). Nickel ions are known to block the T-type calcium channels selectively (Hille, 1992). Jellyfish LVA calcium currents were sensitive to low concentrations of Ni^{2+} ($<100\,\mu mol\,l^{-1}$), which is similar to reports for rat Purkinje cells (Regan, 1991) and amygdaloid neurones (Kaneda and Akaike, 1989). Based upon channel kinetics, activation and inactivation ranges and pharmacological properties, these LVA calcium channels in jellyfish striated muscle cells most closely resemble those of T-type channels.

Possible function of LVA calcium channels in jellyfish striated muscle cells

Due to their low activation threshold and fast inactivation, T-type currents are generally believed to function in combination with other currents to produce pacemaker potentials where rhythmical activity is required (Randall, 1998; Tsien, 1998). In addition, T-type currents are implicated in regulation of cell growth and proliferation (Hermsmeyer, 1998; Triggle, 1998). As the LVA calcium current appears to be the only significant inward current in jellyfish striated muscle cells, this is the first case reported of a LVA calcium current being expressed in isolation without other inward currents. The action potentials of these jellyfish muscles, which have been recorded in current-clamp with sharp electrodes (Spencer, 1978; Spencer and Satterlie, 1981), are reminiscent of those in vertebrate cardiac muscle having large amplitudes (>100 mV) and a long plateau phase (up to 170 ms). Although the ionic basis of the action potential was not clearly established by Spencer and Satterlie, it was demonstrated that most of the inward current was carried by calcium. However, some sodium was required externally to support an action potential. Our results contradict this study; nevertheless it is obvious that the rising phase of the action potential is mostly due to calcium influx through LVA channels, with a delayed repolarisation due to a delayed, rectifier-like potassium current and/or a calcium-dependent potassium current. It must be assumed that the resulting increase in cytoplasmic calcium concentration initiates muscle contraction.

Implications for channel evolution

Due to their phylogenetic position at the base of the metazoan radiation, and being one of the first animal groups to possess sodium currents, cnidarians have been a popular taxon in which to look for ancestral types of sodium channels or hybrid calcium/Na^+ channels (Anderson, 1987; Spafford et al., 1996). Hille (Hille, 1992) noted that T-type calcium channels could be the ancestor of sodium channels, based on the similarity of their kinetics of activation and inactivation. Furthermore, sequence comparisons between sodium and calcium channels show the relatedness of domains in these two channel types (Spafford et al., 1998). Calcium selectivity of HVA channels is conferred by four negatively charged glutamate residues, which form a high-affinity, EDTA-like calcium-binding site in the pore region (Tsien, 1998). This contrasts with sodium channels where two of the negatively charged residues are replaced by a positively charged residue (lysine) and a neutral residue (alanine) (Heinemann et al., 1992; Ellinor et al., 1995). T-type channels might represent the

transition state where these four critical residues are two glutamates and two aspartates (Tsien, 1998). Measurements of sequence similarity between L-type, non-L-type, T-type and sodium channels also suggests that there was an early divergence of these channel types (Tsien, 1998). However, the presence of a functionally undefined, glycosylation-rich, extracellular loop between segments 5 and 6 (located just in front of the pore in domain I and found only in sodium channels and T-type calcium channels) might represent a remnant of their shared ancestry (Spafford et al., 1998).

This jellyfish LVA current activates and inactivates much faster than most vertebrate T-type currents reported to date, with kinetic properties similar to sodium currents. In jellyfish striated muscle cells this calcium current is the major inward current of action potentials, and it is tempting to speculate that this LVA calcium channel is closely related to an ancestral sodium channel.

This article is dedicated to Nikita Grigoriev, a scientist with a technical acumen that, in our experience, was unsurpassed. We thank the staff at Bamfield Marine Station for assistance in collecting jellyfish and Mr R. Bhatnagar and Mr R. Mandryk for technical support. This study was supported by a grant to A.N.S. from the Natural Sciences and Engineering Research Council, Canada.

References

Akaike, N., Kostyuk, P. G. and Osipchuk, Y. V. (1989). Dihydropyridine-sensitive low-threshold calcium channels in isolated rat hypothalamic neurones. *J. Physiol.* **412**, 181–195.

Anderson, P. A. V. (1987). Properties and pharmacology of a TTX-insensitive Na^+ current in neurones of the jellyfish, *Cyanea capillata*. *J. Exp. Biol.* **133**, 233–248.

Apel, E. D., Roberds, S. L., Campbell, K. P. and Merlie, J. P. (1995). Rapsyn may function as a linker between the acetylcholine receptor and the agrin-binding dystrophin-associated glycoprotein complex. *Neuron* **5**, 115–126.

Arnoult, C., Cardullo, R. A., Lemos, J. R. and Florman, H. M. (1996). Activation of mouse sperm T-type Ca^{2+} channels by adhesion to the egg zona pellucida. *Proc. Natl. Acad. Sci. USA* **93**, 13004–13009.

Barish, M. E. (1984). Calcium-sensitive action potential of long duration in the fertilized egg of the ctenophore *Mnemiopsis leidyi*. *Dev. Biol.* **105**, 29–40.

Bean, B. P. (1985). Two kinds of calcium channels in canine atrial cells. *J. Gen. Physiol.* **86**, 1–30.

Berridge, M. J. (1993). Inositol trisphosphate and calcium signalling. *Nature* **361**, 315–325.

Bers, D. M. (1991). *Excitation–Contraction Coupling and Cardiac Contractile Force*, 258 p. Boston: Kluwer Academic Publishers.

Bilbaut, A., Hernandez-Nicaise, M. L., Leech, C. A. and Meech, R. W. (1988). Membrane currents that govern smooth muscle contraction in a ctenophore. *Nature* **331**, 533–535.

Bois, P. and Lenfant, J. (1991). Evidence for two types of calcium currents in frog cardiac sinus venosus cells. *Pflugers Arch.* **417**, 591–596.

Campbell, D. L. and Strauss, H. C. (1995). Regulation of calcium channels in the heart. In *Advances in Second Messenger and Phosphoprotein Research*, Vol. 30 (ed. R. Means), pp. 25–88. New York: Raven Press, Ltd.

Carl, S. L., Felix, K., Caswell, A. H., Brandt, N. R., Brunschwig, J. P., Meissner, G. and Ferguson, D. G. (1995). Immunolocalisation of triadin, DHP receptors, and ryanodine receptors in adult and developing skeletal muscle of rats. *Muscle Nerve* **18**, 1232–1243.

Deitmer, J. (1984). Evidence for two voltage-dependent calcium currents in the membrane of the ciliate *Stylonychia*. *J. Physiol.* **355**, 137–159.

Dubas, F., Stein, P. G. and Anderson, P. A. (1988). Ionic currents of smooth muscle cells isolated from the ctenophore *Mnemiopsis*. *Proc. Roy. Soc. Lond. B* **233**, 99–121.

Ellinor, P. T., Yang, J., Sather, W. A., Zhang, J. F. and Tsien, R. W. (1995). Ca^{2+} channel selectivity at a single locus for high-affinity Ca^{2+} interactions. *Neuron* **15**, 1121–1132.

Ellisman, M. H. and Levinson, S. R. (1982). Immunocytochemical localisation of sodium channel distribution in the excitable membrane of *Electrophorus electricus*. *Proc. Natl. Acad. Sci. USA* **79**, 6701–6711.

Endo, M. (1977). Calcium release from the sarcoplasmic reticulum. *Physiol. Rev.* **57**, 71–108.

Ertel, S. I., Ertel, E. A. and Clozel, J. P. (1997). T-type Ca^{2+} channels and pharmacological blockade: potential pathophysiological relevance. *Cardiovasc. Drugs Ther.* **11**, 723–739.

Grigoriev, N. G., Spafford, J. D., Przysiezniak, J. and Spencer, A. N. (1996). A cardiac-like sodium current in motor neurons of a jellyfish. *J. Neurophysiol.* **76**, 2240–2249.

Hagiwara, N., Irisawa, H. and Kameyama, M. (1988). Contribution of two types of calcium currents to the pacemaker potential of rabbit sino-atrial node cells. *J. Physiol.* **395**, 233–253.

Hagiwara, S. Ozawa, S. and Sand, O. (1975). Voltage clamp analysis of two inward current mechanisms in the egg cell membranes of a star fish. *J. Gen. Physiol.* **65**, 617–644.

Heinemann, S. H., Terlau, H., Imoto, K. and Numa, S. (1992). Calcium channel characteristics conferred on the sodium channel by single mutations. *Nature* **356**, 441–443.

Hermsmeyer, K. (1998). Role of T channels in cardiovascular function. *Cardiology* **89**, 2–9.

Hille, B. (1992). *Ionic Channels of Excitable Membranes*, 607 p. Sunderland: Sinauer.

Hirano, Y., Fozzard, H. A. and January, C. T. (1989). Characteristics of L- and T-type Ca^{2+} currents in canine cardiac Purkinje fibers. *Am. J. Physiol.* **256**, 1478–1492.

Huguenard, N. J. (1996). Low-threshold calcium currents in central nervous system neurons. *Ann. Rev. Physiol.* **58**, 329–348.

Kaneda, M. and Akaike, N. (1989). The low-threshold Ca^{2+} current in isolated amygdaloid neurons in the rat. *Brain Res.* **497**, 187–190.

Kaneda, M., Ito, C. and Akaiko, N. (1990). Low-threshold calcium current in isolated Purkinje cell bodies of rat cerebellum. *J. Neurophysiol.* **63**, 1046–1051.

Kirsch, J., Wolters, I., Triller, A. and Betz, H. (1993). Gephyrin antisense oligonucleotide prevents glycine receptor clustering in spinal neurones. *Nature* **366**, 745–748.

Lievano, A., Santi, C. M., Serrano, C. J., Trevino, C. L., Bellve, A. R., Hernandez-Cruz, A. and Darszon, A. (1996). T-type Ca^{2+} channels and alpha 1E expression in spermatogenic cells, and their possible relevance to the sperm acrosome reaction. *FEBS Lett.* **388**, 150–154.

Lin, Y.-C. J., Grigoriev, N. G. and Spencer, A. N. (2000). Wound healing in jellyfish striated muscle involves rapid switching between two modes of cell motility and a change in the source of regulatory calcium. *Dev. Biol.* **225**, 87–100.

Lin, Y.-C. J. and Spencer, A. N. (2001). Localisation of intracellular calcium stores in the striated muscles of the jellyfish *Polyorchis penicillatus*: possible involvement in excitation–contraction coupling. *J. Exp. Biol.* **204**, 3727–3736.

Lupa, M. T. and Caldwell, J. M. (1994). Sodium channels aggregate at former synaptic sites in innervated and denervated regenerating muscles. *J. Cell Biol.* **124**, 139–147.

Mackie, G. O. and Meech, R. W. (1985). Separate sodium and calcium spikes in the same axon. *Nature* **313**, 791–793.

Ödblom, M. P., Williamson, R. and Jones, M. B. (2000). Ionic currents in cardiac myocytes of squid, *Alloteuthis subulata*. *J. comp. Physiol. B* **170**, 11–20.

Plickert, G. and Kroiher, M. (1988). Proliferation kinetics and cell lineages can be studied in whole mounts and macerates by means of BrdU/anti-BrdU technique. *Development* **103**, 791–794.

Przysiezniak, J. and Spencer, A. N. (1992). Voltage-activated calcium currents in identified neurons from a hydrozoan jellyfish, *Polyorchis penicillatus*. *J. Neurosci.* **12**, 2065–2078.

Randall, A. D. (1998). The molecular basis of voltage-gated Ca^{2+} channel diversity: is it time for T? *J. Membr. Biol.* **161**, 207–213.

Randall, A. D. and Tsien, R. W. (1997). Contrasting biophysical and pharmacological properties of T-type and R-type calcium channels. *Neuropharmacology* **36**, 879–893.

Regan, L. J. (1991). Voltage-dependent calcium currents in Purkinje cells from rat cerebellar vermis. *J. Neurosci.* **11**, 2259–2269.

Richard, S., Diochot, S., Nargeot, J., Baldy-Moulinier, M. and Valmier, J. (1991). Inhibition of T-type calcium currents by dihydropyridines in mouse embryonic dorsal root ganglion neurons. *Neurosci. Lett.* **132**, 229–234.

Ritchie, J. M. and Rogart, R. B. (1977). Density of sodium channels in mammalian myelinated nerve fibers and nature of the axonal membrane under the myelin sheath. *Proc. Natl. Acad. Sci. USA* **74**, 211–215.

Santi, C. M., Darszon, A. and Hernandez-Cruz, A. (1996). A dihydropyridine-sensitive T-type Ca^{2+} current is the main Ca^{2+} current carrier in mouse primary spermatocytes. *Am. J. Physiol.* **271**, 1583–1593.

Schmid, V., Stidwill, R., Bally, A., Marcum, B. and Tardent, P. (1981). Heat dissociation and maceration of marine cnidarians. *Roux's Arch. Dev. Biol.* **190**, 143–149.

Schild, D., Geiling, H. and Bischofberger, J. (1995). Imaging of L-type Ca^{2+} channels in olfactory bulb neurones using fluorescent dihydropyridine and a styryl dye. *J. Neurosci. Meth.* **59**, 183–190.

Spafford, J. D., Grigoriev, N. G. and Spencer, A. N. (1996). Pharmacological properties of voltage-gated sodium currents in motor neurones from a jellyfish *Polyorchis penicillatus*. *J. Exp. Biol.* **199**, 941–948.

Spafford, J. D., Spencer, A. N. and Gallin, W. J. (1998). A putative voltage-gated sodium channel α subunit (PpSCN1) from the hydrozoan jellyfish, *Polyorchis penicillatus*: structural comparisons and evolutionary considerations. *Biochem. Biophys. Res. Comm.* **244**, 772–780.

Spencer, A. N. (1978). Neurobiology of *Polyorchis*. I. Function of effector systems. *J. Neurobiol.* **9**, 143–157.

Spencer, A. N. (1979). Neurobiology of *Polyorchis*. II. Structure of effector systems. *J. Neurobiol.* **10**, 95–117.

Spencer, A. N. and Satterlie, R. A. (1981). The action potential and contraction in subumbrellar swimming muscle of *Polyorchis penicillatus* (Hydromedusae). *J. Comp. Physiol.* **144**, 401–407.

Srinivasan, Y., Elmer, L. W., Davis, J. Q., Bennett, V. and Angelides, K. J. (1988). Ankyrin and spectrin associate with voltage-dependent sodium channels in brain. *Nature* **333**, 177–180.

Takahashi, K. and Akaike, N. (1991). Calcium antagonist effects on low threshold (T-type) calcium current in rat isolated hippocampal CA1 pyramidal neurons. *J. Pharm. Exp. Ther.* **256**, 169–175.

Triggle, D. J. (1998). The physiological and pharmacological significance of cardiovascular T-type, voltage-gated calcium channels. *Am. J. Hypertns.* **11**, 80–87.

Tseng, G. N. and Boyden, P. A. (1989). Multiple types of Ca^{2+} currents in single canine Purkinje cells. *Circ. Res.* **65**, 1735–1750.

Tsien, R. W. (1998). Key clockwork component cloned. *Nature* **391**, 839–841.

Wang, H., Bedford, F. K., Brandon, N. J., Moss, S. J. and Olsen, R. W. (1999). $GABA_A$-receptor-associated protein links $GABA_A$ receptors and the cytoskeleton. *Nature* **397**, 69–72.

Yamoah, E. N. and Crow, T. (1994). Two components of calcium currents in the soma of photoreceptors of *Hermissenda*. *J. Neurophysiol.* **72**, 1327–1336.